ISSN 0030-400X, Optics and Spectroscopy, 2018, Vol. 124, No. 6, pp. 808–813. © Pleiades Publishing, Ltd., 2018.
Original Russian Text © V.N. Kruchinin, V.A. Volodin, T.V. Perevalov, A.K. Gerasimova, V.Sh. Aliev, V.A. Gritsenko, 2018, published in Optika i Spektroskopiya, 2018, Vol. 124, No. 6, pp. 777–782.

CONDENSED-MATTER SPECTROSCOPY

Optical Properties of Nonstoichiometric Tantalum Oxide TaO_x ($x < 5/2$) According to Spectral-Ellipsometry and Raman-Scattering Data

V. N. Kruchinin[a, *], V. A. Volodin[a, b], T. V. Perevalov[a, b], A. K. Gerasimova[a], V. Sh. Aliev[a], and V. A. Gritsenko[a, b, c]

[a] *Rzhanov Institute of Semiconductor Physics, Siberian Branch, Russian Academy of Sciences, Novosibirsk, 630090 Russia*

[b] *Novosibirsk State University, Novosibirsk, 630090 Russia*

[c] *Novosibirsk State Technical University, Novosibirsk, 630073 Russia*

**e-mail: kruch@isp.nsc.ru*

Received February 10, 2018

Abstract—Optical properties of amorphous nonstoichiometric tantalum-oxide films of variable composition (TaO_x, $x = 1.94–2.51$) in the spectral range of 1.12–4.96 eV, obtained by ion-beam sputtering-deposition of metallic tantalum at different partial oxygen pressures ($0.53–9.09 \times 10^{-3}$ Pa), have been investigated. It is shown by spectral ellipsometry that the character of dispersion of the absorption coefficient and refractive index in TaO_x of variable composition suggests that light-absorbing films with dispersion similar to that in metals are formed at oxygen pressures in the growth chamber below 2.21×10^{-3} Pa, whereas transparent films with dielectric dispersion are formed at pressures above 2.81×10^{-3} Pa. According to the data of quantum-chemical simulation, the absorption peak at a photon energy of 4.6 eV in TaO_x observed in the absorption-coefficient dispersion spectrum is due to oxygen vacancy. The peak in the Raman-scattering spectra of TaO_x films with metallic dispersion at frequencies of 200–230 cm^{-1} is presumably related to tantalum nanoclusters.

DOI: 10.1134/S0030400X18060140

INTRODUCTION

Tantalum-oxide (Ta_2O_5) films are characterized by high permittivity (20–50) and used as insulators in the storage capacitors of dynamic storage devices [1–4]. In addition, Ta_2O_5 films are used as storage medium instead of silicon nitride in flash memory [5]. The use of nonstoichiometric tantalum oxide ($TaO_{x<5/2}$) films as storage medium in nonvolatile high-speed resistive flash memory is of great interest [6]. A change in the chemical composition (stoichiometry) of TaO_x changes its electronic structure, which makes it possible to control the physical (optical and electric) properties of the layer. The purpose of this study was to analyze the optical properties of nonstoichiometric $TaO_{x<5/2}$ films by spectral ellipsometry, Raman-scattering spectroscopy, and quantum-chemical simulation.

EXPERIMENTAL

Samples

The samples for study were prepared by ion-beam sputtering deposition (IBSD). A series of TaO_x films of variable composition ($x < 5/2$) 10–50 nm thick were grown on KEF-4.5 Si(100) substrates (n-Si:P with a resistivity of 4.5 Ω cm). Before the growth, a native oxide layer was removed from the silicon substrates in a hydrofluoric acid (HF) solution. The sputtering was performed using a metal tantalum (Ta) target. The target was sputtered by Ar^+ ions with an energy of 1.2 keV with simultaneous inlet of high-purity oxygen ($[O_2] > 99.999\%$) into the chamber. Partial oxygen pressure P_{O_2} in the growth zone was varied in the range of $0.53–9.09 \times 10^{-3}$ Pa, which made it possible to form TaO_x films of variable compositions, both stoichiometric ($x \approx 5/2$) and nonstoichiometric ($x < 5/2$) (Table 1). The x value was determined using the previously obtained calibration curve of the dependence of x ($x = [O]/[Ta]$ is the ratio of elemental atomic fractions obtained based on X-ray photoelectron spectroscopy (XPS)) on the oxygen pressure [7].

The comparative analysis within ellipsometric measurements was performed using metallic tantalum samples (tantalum foil of TVCh grade) $8 \times 8 \times 0.5$ mm in size preliminarily subjected to mechanical polishing and cleaning in boiling toluene.

Table 1. Synthesis conditions, composition, and optical properties of the TaO_x films

Sample no.	$P_{O_2} \times 10^3$, Pa	x in TaO_x, according to the XPS data	Film thickness, nm, according to spectral-ellipsometry data	Optical properties of TaO_x according to ellipsometry data (at $E = 1.96$ eV)	
				n	$\alpha \times 10^6$, cm^{-1}
T1	0.53	1.94	24.3	3.614	0.510
T2	1.08	1.99	11.2	3.057	0.406
T3	1.35	2.13	11.7	2.792	0.307
T4	1.71	2.22	46.7	2.692	0.242
T5	2.21	2.44	53.1	2.530	0.137
T6	2.81	2.53	44.4	2.476	–
T7	3.49	2.51	50.2	2.246	–
T8	9.09	2.59	53.0	2.089	–
Met.	–	–	–	1.734	0.414

Ellipsometry

For ellipsometric analysis of the system, we used the data obtained by an ELLIPS-1891-SAG spectral ellipsometer (Rzhanov Institute of Semiconductor Physics, Siberian Branch, Russian Academy of Sciences) [8]. The spectral dependences of ellipsometric angles $\Psi(E)$ and $\Delta(E)$ were measured in the photon-energy range of 1.12–4.96 eV. The spectral instrumental resolution was ~0.01 eV, the recording time for one spectrum did not exceed 20 s, and the angle of incidence of light on the sample was 70°. The four-band measurement technique with subsequent averaging over all four bands was used.

Recorded spectra $\Psi(E)_{exp}$ and $\Delta(E)_{exp}$ were used afterward for solving the inverse ellipsometry problem (IEP) and fitting the calculated spectral dependences of ellipsometric angles $\Psi(E)_{calc}$ and $\Delta(E)_{calc}$ to the experimental ones in accordance with the fundamental equation of ellipsometry

$$e^{i\Delta} \tan \Psi = \frac{R_p}{R_s}, \quad (1)$$

where R_p and R_s are the complex reflectances for waves polarized in the plane of incidence and perpendicular to it, which depend on the optical constants and layer thicknesses.

For ellipsometric calculations, we used the optical model of single-layer reflecting system; the film thicknesses and dependences $n(E)$ and $\alpha(E)$ were calculated as follows.

(i) Transparent films (T6–T8). The fitting of the spectral dependences of the polarization angles in the entire spectral range for m spectral points was performed using minimization of the error function:

$$\sigma^2 = \frac{1}{m}\sum_{i=1}^{m}[(\Delta_{exp} - \Delta_{calc})^2 + (\Psi_{exp} - \Psi_{calc})^2], \quad (2)$$

where Ψ_{exp} (Ψ_{calc}) and Δ_{exp} (Δ_{calc}) are the experimental (calculated) values of ellipsometric angles Ψ and Δ, respectively. The thickness and dispersion relation $n(E)$ for transparent TaO_x films were found simultaneously; dependence $n(E)$ was calculated based on the Cauchy polynomial dependence [9, 10]:

$$n(\lambda) = a + \frac{b}{\lambda^2} + \frac{c}{\lambda^4}, \quad (3)$$

where a, b, and c are the fitting coefficients.

(ii) Light-absorbing films (T1–T5). The n and α values were found independently at each spectrum point. The thicknesses of opaque TaO_x films were determined using separate multiple-angle measurements on an LEF-3M ellipsometer at the angles of incidence of light on the sample of 50°, 60°, and 70°; the wavelength was $\lambda = 632.8$ nm.

The silicon optical characteristics were taken for the calculations from the Adachi database [11].

Raman Spectroscopy

The structural properties of the initial TaO_x films were investigated by Raman-scattering spectroscopy. Raman spectra were recorded at room temperature in backscattering geometry; the excitation was performed using the Ar^+-laser line with a wavelength of 514.5 nm; the polarization of the scattered light was not analyzed. We used a T64000 spectrometer (Horiba Jobin Yvon). The spectral resolution did not exceed 2 cm^{-1}. An attachment for microscopic investigations of Raman light scattering was applied. The laser-beam power was 2 mW on the sample surface. To minimize the structure heating under the laser beam, the sample was placed slightly below the focus (the focal spot size was ~8 μm).

Quantum-Chemical Calculations

The quantum-chemical simulation of the electronic structure of tantalum oxide was performed in the Quantum-ESPRESSO program package within the density functional theory in the model of periodic supercells [12]. The calculations were performed for the orthorhombic λ-Ta_2O_5 phase because, for this crystalline modification, the electronic structures of the bulk and oxygen vacancies are the same as for amorphous tantalum oxide [13, 14]. In the λ-Ta_2O_5 structure, Ta atoms have the coordination number of 6, while O atoms are of three types: with twofold and threefold coordinations in the Ta atomic plane and with twofold coordination in the oxygen atomic plane. The twofold-coordinated O vacancy in the Ta plane has the minimum energy of oxygen-vacancy formation. We used the hybrid Becke–Lie–Yang–Parr exchange-correlation functional B3LYP. The wave functions of valence electrons were expanded in basis of the plane waves with a cutoff energy of 950 eV; the core was taken into account via norm-retaining pseudopotentials. The cutoff energy was chosen so as to obtain convergence with respect to the total cell energy of no worse than 0.006 eV/atom. The calculations were performed using the electronic configurations $[Xe]5d^36s^26p^0$ for Ta and $[He]2s^22p^4$ for O. Oxygen vacancies were formed by removing oxygen from the supercell obtained by 2 × 2 × 3 translation along the crystallographic axes of 14-atom unit cells with subsequent relaxation of all atoms with the force-convergence threshold of 0.04 eV/Å.

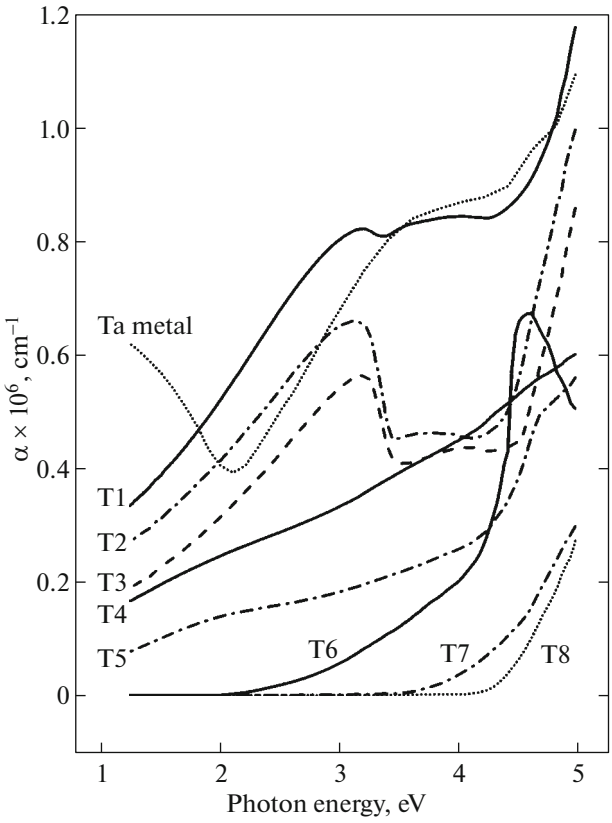

Fig. 1. Spectral dependence of the absorption coefficient of TaO_x films of variable composition and metallic Ta.

RESULTS AND DISCUSSION

Dispersion of Optical Constants Based on the Spectral-Ellipsometry Data

Figure 1 shows the spectral dependence of the TaO_x absorption coefficient. The absorption edge of stoichiometric Ta_2O_5 (sample T8) is at 4.2 eV. This value was previously determined for Ta_2O_5 in [15]. Enrichment of TaO_x in metal is accompanied by a low-energy shift of the fundamental absorption edge. The absorption edge for sample T7 is at 2.5 eV, whereas for sample T6 it shifts to ~2.0 eV. The spectral dependence of the TaO_x absorption coefficient has a complex character. At a high degree of oxygen depletion, the TaO_x dispersion spectra exhibit specific features similar to those for metallic tantalum. The absorption peak at 4.6 eV occurs in sample T6. In samples T5 and T4, one can observe kinks at an energy close to 4.6 eV.

To reveal the nature of the absorption peak at 4.6 eV in sample T6, we performed quantum-chemical simulation of the electronic structure of an isolated oxygen vacancy with the minimum formation energy in the 168-atom λ-Ta_2O_5 supercell. The calculated spectra of the partial density of electronic states (PDES), which are closest to the oxygen vacancy of Ta atoms, show that the vacancy forms an occupied defect state in the band gap at 2.4 eV above the top of the valence band (Fig. 2). The defect state is formed mainly by Ta 5*d* electrons with a significant contribution from Ta 6*s* and Ta 6*p*. The calculated spectrum predicts the possibility of optical transitions at the O vacancy with energies of 4.5 and 4.65 eV from the defect level in the band gap to Ta 6*p*/Ta 6*s* and Ta 5*d* states in the conduction band, respectively. The energies of these transitions are in agreement with the experimental optical-absorption peak at 4.6 eV of amorphous TaO_x for sample T6. It is noteworthy that the calculations also predict transitions with energies of 3.65 and 5.27 eV. The TaO_x optical-absorption spectra exhibit no specific features for these photon energies most likely due to a small value of the transition matrix elements.

Figure 3 shows the dispersion of the refractive index of TaO_x of variable composition. The films with a low content of excess metal exhibit normal dispersion. The refractive index increases with an increase in the photon energy. The TaO_x films with a high content of excess metal are characterized by anomalous dispersion. The refractive index decreases with an increase in the photon energy at low photon energies, whereas at high photon energies it increases. In the films strongly depleted of oxygen, the behavior of the

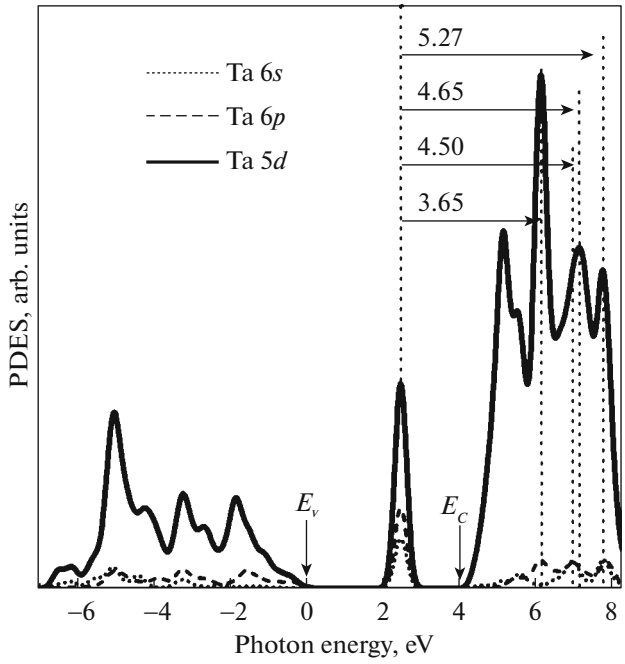

Fig. 2. Partial density of electronic states (PDES) of Ta atoms, which are closest to the neutral O vacancy, in the 168-atom λ-Ta_2O_5 supercell: Ta 5*d* (solid curve), Ta 6*p* (dashed curve), and Ta 6*s* (dotted curve). The top of valence band E_v is at the zero energy.

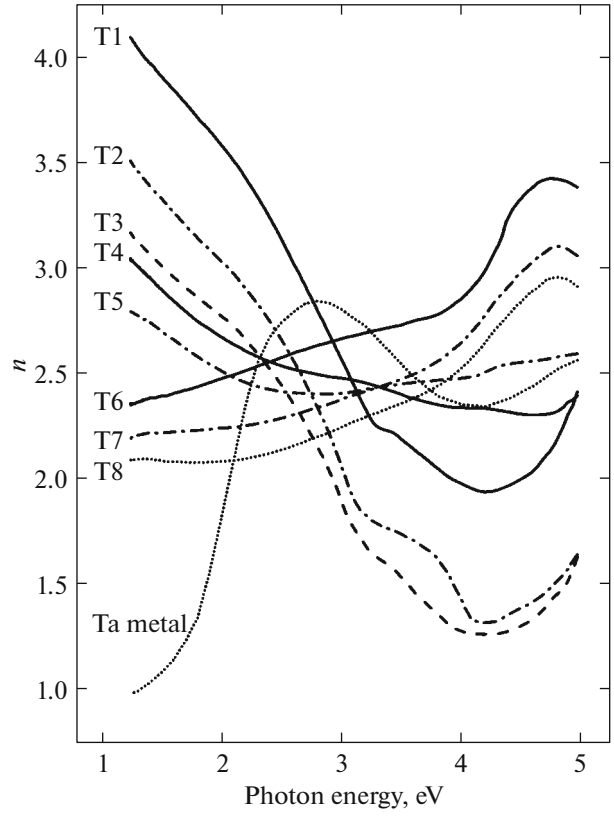

Fig. 3. Spectral dependence of the refractive index of the TaO_x films of variable composition.

spectral dependence of the refractive index at photon energies in the range of 3–5 eV is close to that for the metal. In the low-energy region, at photon energies of less than 3 eV, the refractive index in the metal decreases from 2.8 to 1.0. In the TaO_x samples strongly depleted of oxygen (T1–T5), the refractive index increases (in contrast to the metal) in magnitude in the photon-energy range of 3.0–1.3 eV. Determination of the reasons for the phenomenon observed calls for further investigations.

Raman Spectroscopy

Figure 4 shows the Raman spectra of the TaO_x film (gray curve, sample T1, Table 1) and silicon substrate (black curve). The main signal in the Raman spectra related to the silicon substrate is the 520.6-cm^{-1} line corresponding to the long-wavelength optical phonon. For improved readability, the vertical scale is bounded and this peak is cut off. In addition, the spectrum of single-crystal silicon has specific features related to two-phonon scattering: two acoustic phonons (~300 cm^{-1}), optical and acoustic phonons (~650 cm^{-1}), and two optical phonons (~970 cm^{-1}).

The TaO_x film is semitransparent in the visible spectral range at the thickness under consideration, and its spectrum also exhibits the signal from the substrate. The narrow peaks at frequencies lower than

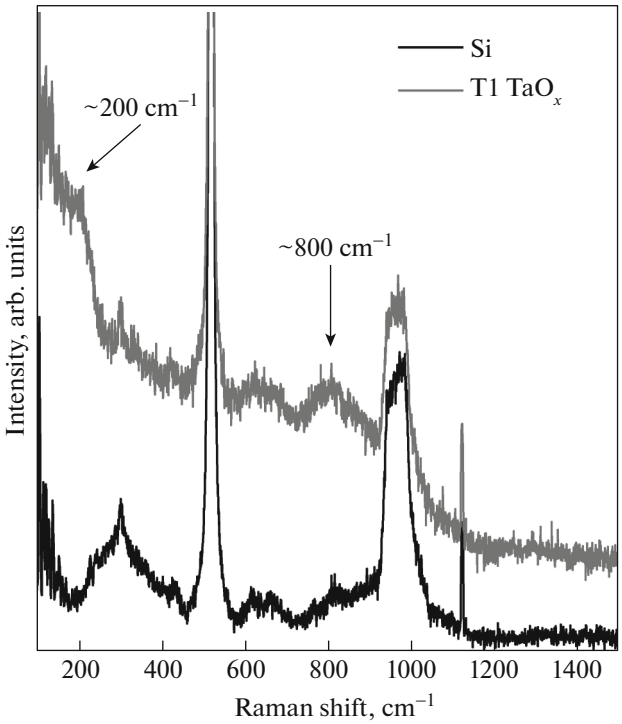

Fig. 4. Raman spectra of the TaO_x film (T1) and Si substrate.

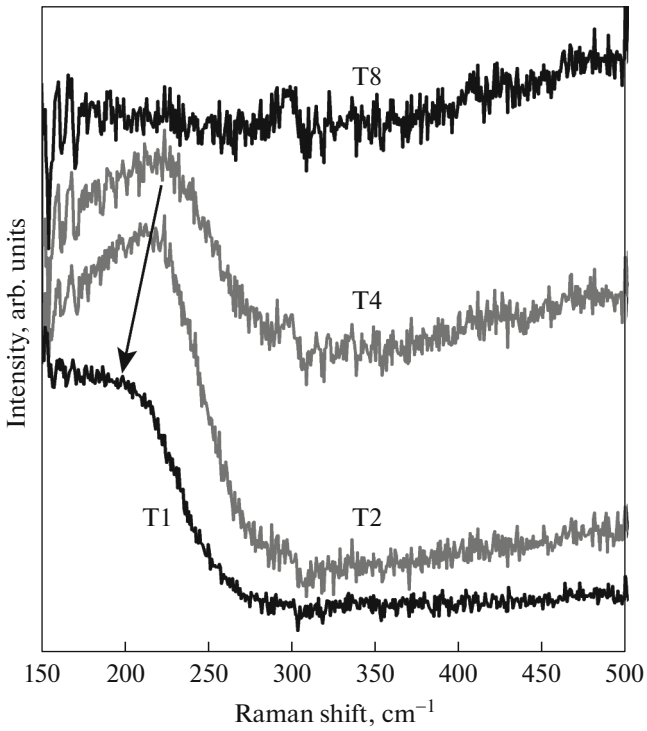

Fig. 5. Raman spectra of the TaO_x films (T1–T4). The contribution from the Si substrate is subtracted.

150 cm^{-1} are the result of inelastic light scattering from molecules contained in air. The TaO_x film spectrum also includes specific features at ~200 and ~800 cm^{-1}. Raman spectra of amorphous Ta_2O_5 are known to contain specific feature related to the maximum in the density of vibrational states in range from 600 to 1000 cm^{-1} [16–20]. This corresponds to the vibrational frequencies of tantalum–oxygen bonds. The ~800-cm^{-1} peak in the spectrum of sample T1 is likely due to scattering from vibrations of these bonds.

To reveal the nature of the peak in the acoustic spectral region (~200 cm^{-1}), we measured the Raman spectra of the films prepared at different partial oxygen pressures. Figure 5 shows the Raman spectra of the TaO_x films (samples T1–T4, see Table 1), from which the silicon-substrate spectrum is subtracted. The spectra obtained exhibit specific features in the frequency range of ~200 cm^{-1}. This specific feature was also observed in [16] upon decreasing oxygen content in the TaO_x films with different stoichiometric compositions. This feature may presumably correspond to the contribution from phonons, localized in tantalum nanoclusters, or surface phonons at the boundary of tantalum clusters. One can see that this acoustic peak increases and shifts with a decrease in the partial oxygen pressure. Only sample T4 stands out from the general dependence. This question requires further investigation. Thus, the occurrence of the acoustic "shoulder" can be related to the presence of tantalum clusters in the films.

Thus, the optical properties and structure of tantalum-oxide (TaO_x) films of variable composition were studied by spectral ellipsometry and Raman spectroscopy. Depending on the oxygen content, the TaO_x films have dispersions of optical constants $n(E)$ and $\alpha(E)$ similar to those in metals (which can be due to the presence of Ta clusters) or are transparent films ($\alpha(E) = 0$) with dispersion of $n(E)$ of the normal dielectric type. A peak at an energy of 4.6 eV is observed in spectra $\alpha(E)$ for the TaO_x films slightly enriched in metal. According to the data of quantum-chemical simulation, this peak is due to optical transitions at the oxygen vacancy. The peaks at ~800 and 200–230 cm^{-1} in the Raman spectra indicates the presence of the Ta_2O_5 stoichiometric phase and Ta metal clusters in the TaO_x films.

ACKNOWLEDGMENTS

This study was supported by state contract no. 0306-2016-0004. The quantum-chemical simulation was performed on the equipment of the Siberian Supercomputer Center of Collective Use of the Institute of Computational Mathematics and Mathematical Geophysics, Siberian Branch, Russian Academy of Sciences.

REFERENCES

1. G. D. Wilk, R. M. Wallace, and J. M. Anthony, J. Appl. Phys. **89**, 5243 (2001). doi 10.1063/1.1361065
2. J. Robertson, Eur. Phys. J. Appl. Phys. **28**, 265 (2004). doi 10.1051/epjap:2004206
3. T. V. Perevalov and V. A. Gritsenko, Phys. Usp. **50**, 561 (2007). doi 10.3367/UFNr.0180.201006b.0587
4. J. Robertson and R. M. Wallace, Mater. Sci. Eng. R **88**, 1 (2015).
5. H. Zhu, J. E. Bonevich, H. Li, C. A. Richter, H. Yuan, O. Kirillov, and Q. Li, Appl. Phys. Lett. **104**, 233504 (2014). doi 10.1063/1.4883717
6. M.-J. Lee, C. B. Lee, D. Lee, S. R. Lee, M. Chang, J. H. Hur, Y.-B. Kim, C. J. Kim, D. H. Seo, S. Seo, U.-I. Chung, I.-K. Yoo, and K. Kim, Nat. Mater. **10**, 625 (2011). doi 10.1038/NMAT3070
7. V. A. Gritsenko, T. V. Perevalov, V. A. Voronkovskii, A. A. Gismatulin, V. N. Kruchinin, V. Sh. Aliev, V. A. Pustovarov, I. P. Prosvirin, and Y. Roizin, ACS Appl. Mater. Interfaces (2018, in press). doi 10.1021/acsami.7b16753
8. S. V. Rykhlitskii, E. V. Spesivtsev, V. A. Shvets, and V. Yu. Prokop'ev, Prib. Tekh. Eksp. **2**, 161 (2012).
9. H. Tompkins and E. A. Irene, *Handbook of Ellipsometry* (William Andrew, Springer, Berlin, 2005).
10. V. A. Shvets, V. N. Kruchinin, and V. A. Gritsenko, Opt. Spectrosc. **123**, 728 (2016). doi 10.7868/S0030403417110204

11. S. Adachi, *Optical Constants of Crystalline and Amorphous Semiconductors: Numerical Data and Graphical Information* (Springer, New York, 1999).

12. P. Giannozzi, S. Baroni, N. Bonini, M. Calra, R. Car, C. Cavazzoni, D. Ceresoli, G. L. Chiarotti, M. Cococcioni, I. Dabo, et al., J. Phys.: Condens. Matter **21**, 395502 (2009). doi 10.1088/0953-8984/21/39/395502

13. S. H. Lee, J. Kim, S. J. Kim, S. Kim, and G. S. Park, Phys. Rev. Lett. **110**, 235502 (2013). doi 10.1103/PhysRevLett.110.235502

14. Y. Z. Guo and J. Robertson, Microelectron. Eng. **147**, 254 (2015). doi 10.1016/j.mee.2015.04.065

15. V. A. Shvets, V. S. Aliev, D. V. Gritsenko, S. S. Shaimeev, E. V. Fedosenko, S. V. Rykhlitski, V. V. Atuchin, V. A. Gritsenko, V. M. Tapilin, and H. Wong, J. Non-Cryst. Solids **354**, 3025 (2008). doi 10.1016/j.jnoncrysol.2007.12.013

16. T. Tsuchiya, H. Imai, S. Miyoshi, P. A. Glans, J. Guo, and S. Yamaguchi, Phys. Chem. Chem. Phys. **13**, 17013 (2011). doi 10.1039/c1cp21310e

17. C. Joseph, P. Bourson, and M. D. Fontana, J. Raman Spectrosc. **43**, 1146 (2012). doi 10.1002/jrs.3142

18. U. Balachandran and N. G. Eror, Mater. Res. Bull. **17**, 219 (1982).

19. U. Balachandran and N. G. Eror, J. Less-Common Met. **84**, 291 (1982).

20. P. S. Dobal, R. S. Katiyar, Y. Jiang, R. Guo, and A. S. Bhalla, J. Raman Spectrosc. **31**, 1061 (2000).

Translated by A. Sin'kov